Molecular Transport Effects in Turbulent Diffusion Flames at Moderate Reynolds Number

R. W. Bilger*

The University of Sydney, New South Wales, Australia

In flames, molecular diffusivities are enhanced by the high temperatures and can be of the same order as turbulent diffusivities in flames of moderate Reynolds number. A perturbation analysis is used to quantify effects in a hydrogen/air diffusion flame which arise from differential molecular diffusivities. The analysis uses perturbations about the equal diffusivity, adiabatic, equilibrium theory commonly used and yields solutions for the average and higher moments for the departures in normalized element mass fractions and enthalpy. The results are compared with laser-Raman measurements of Drake et al. in a relatively low Reynolds number flame. Generally the agreement is excellent.

Introduction

IN theoretical models[1-3] of turbulent diffusion flames, great simplifications are introduced by the assumption that the mass diffusivities of all species are equal and are equal to the thermal diffusivity; that is, all Lewis numbers are unity. It can then be shown[4] that the elemental composition and enthalpy at any point in the fluid is the same as that obtained by mixing a mass ξ of the unmixed fuel with a mass $1 - \xi$ of the unmixed oxidant. The mixture fraction $\xi = \xi(x,t)$ is then the only variable needed to describe the state of mixing. No differential (or "preferential") diffusion of species or enthalpy has occurred and the elemental mass fractions and the enthalpy are linearly related to ξ and to one another.

In practical flames, molecular diffusivities are seldom equal and resort is made to the argument[5] that if the Reynolds number of the turbulence is high enough, molecular effects will be confined to the high wavenumber end of the spectrum. There will be no significant effect on the main quantities of interest, such as the mean concentrations and temperature, and the variances and covariances of the concentration and temperature fluctuations; these quantities are associated with the low wavenumber, "energy-containing" range of the turbulence spectrum. As a consequence the mixture fraction concept remains valid as far as the main features of theoretical models are concerned.

In labortory flames turbulence Reynolds numbers are seldom very high. In nonreacting flows in the laboratory, turbulence Reynolds numbers are relatively modest, but they are, in general, sufficient to ensure a separation of the energy-containing and dissipation ranges of the turbulence spectrum. At flame temperatures, however, the kinematic viscosity is increased tenfold or more and turbulence Reynolds numbers are correspondingly lowered. Furthermore, the diffusivities of some species such as molecular and atomic hydrogen are so much higher than the kinematic viscosity that it can be expected that molecular transport will have even greater effects on the low wavenumber end of the spectrum for hydrogen containing species. Thus one might expect to find significant effects of molecular transport on means and variances of quantities such as concentration and temperature in laboratory flames.

Recent measurements by Drake et al.[6,7] in a hydrogen diffusion flame of modest Reynolds number show a significant departure from what is expected from equal diffusivity theory. They have used pulsed laser Raman spectroscopy to obtain simultaneous measurements of temperature and nitrogen and hydrogen concentration with excellent spatial and temporal resolution. Correlation plots of concentration vs temperature for these two species show considerable departure from the curve that is obtained assuming equal diffusivities, adiabaticity and chemical equilibrium. Predicted departures from adiabaticity and chemical equilibrium are not qualitatively or quantitatively consistent with the measurements. The measurements do, in general, lie between the equal diffusivity curve and calculations made by Miller and Kee[8] for a laminar flame. Differential diffusion effects are significant in the laminar flame, and Drake et al.[6] consider that such effects are the explanation for their measurements.

A theoretical model for predicting differential diffusion effects in turbulent diffusion flames is presented here. It is used to predict the departures from the equal diffusivity theory for the conditions of the Drake et al.[6] flame. It could also be used to predict the effects of differential diffusion, or Reynolds number, on nitric oxide formation in such flames, a question that has been raised in earlier work.[9] Other uses of such a model include the prediction of the extent of differential diffusion between the fuel and seed particles put into the flow to act as a fuel tracer in the so-called marker nephelometry technique.[10,11] Such studies are planned for the future.

In earlier papers[12,13] the theory for differential diffusion in nonreacting flows has been developed. An equation is derived for a variable, z, which is the difference between mixture fractions defined for various species. This parameter is then a direct measure of differential diffusion effects and has zero values in both the unmixed fluids. Its only source is a source term involving the difference, d, in the diffusion coefficients for the species and the mean gradient of a mixture fraction. It is shown that a characteristic scale for the amount of differential diffusion z_0 is related to the characteristic scale of the mixture fraction ξ_0 and the turbulent diffusivity D_T by

$$z_0 \sim - \frac{d}{(D_T + D)} \xi_0 \tag{1}$$

where D is the actual molecular diffusivity for the species. Since the turbulent diffusivity increases with turbulence Reynolds number $Re_t (\equiv u'L/\nu$, where u' is the rms velocity fluctuation, L the integral length scale of the turbulence, and ν the kinematic viscosity) the asymptotic behavior at high

Reynolds number is

$$z_0 \propto 1/Re_t$$

which is consistent with our notions that the effects will only be important at low Reynolds number.

In chemically reacting systems this approach is complicated by the fact that conserved scalars, such as elemental mass fractions and enthalpy, are dependent on many molecular species concentrations and the temperature, each with its own effective diffusivity. Moreover, the relative proportions of the species change and it is not possible to derive a simple weighting for these diffusivities directly. It was thought earlier[12] that this problem could be overcome by an appropriate scaling in the reaction zone, but this approach has not proved fruitful. In this paper a different approach is adopted. Molecular species concentrations and temperature are related directly to the mixture fraction (the equal diffusivity, adiabatic, chemical equilibrium relations) with linear perturbations for the effects of differential diffusion. It is then possible to define effective diffusivities and differential diffusivities for elemental species and enthalpy and to formulate equations for their differences or perturbations in their mixture fractions.

In the next section the theory is developed. This is followed by presentation of the effective diffusivities and other properties computed for the hydrogen-air system. The modeled turbulence equations are then solved numerically for the Drake et al.[6] flame conditions and the results compared with the experiment.

Theory

In the absence of significant body force and viscous contributions to the energy balance, the species balance and energy equations may be written[14,15]

$$\rho \frac{DY_i}{Dt} = w_i - \nabla \cdot j_i \tag{2}$$

$$\rho \frac{Dh}{Dt} = -\nabla q + \frac{Dp}{Dt} - \rho \phi_r \tag{3}$$

where Y_i and w_i are the mass fraction and volumetric reaction rate of species i, and j_i its mass flux relative to the overall mass flux of the fluid; ρ is the density, p the fluid pressure, and h the enthalpy (including enthalpy of formation) given by

$$h \equiv \sum_{i=1}^{N} Y_i \left(h_i^0 + \int_{T_0}^{T} c_{p_i} dT \right) \equiv \sum_{i=1}^{N} Y_i h_i \tag{4}$$

where c_{p_i} and h_i^0 are the specific heat at constant pressure and the enthalpy of formation of species i, and ϕ_r the rate of radiative loss per unit mass, respectively. Neglecting thermal diffusion contributions to the heat flux vector q, this may be written

$$q = -\lambda \nabla T + \sum_{i=1}^{N} j_i h_i \tag{5}$$

with λ the thermal conductivity and T the temperature. The dilute species approximation is adopted for the diffusional fluxes j_i so that they have the Fick's law form

$$j_i = -\rho D_i \nabla Y_i \qquad i = 1\text{-}(N-1)$$

$$= \sum_{k=1}^{N-1} \rho D_k \nabla Y_k \qquad i = N \tag{6}$$

where D_i is the diffusivity of species i into the diluent species N, here assumed to be nitrogen. Note that Eqs. (6) preserve continuity; this is not achieved if a Fick's law approximation is used for the diluent species N. On substituting Eqs. (6) into Eq. (5) we obtain

$$q = -\lambda \nabla T + \sum_{i=1}^{N-1} \rho D_i (h_i - h_N) \nabla Y_i$$

Using this and Eqs. (6) in Eqs. (2) and (3), and neglecting the substantial derivative of the pressure, we obtain self-consistent equations for species and enthalpy:

$$\rho \frac{DY_i}{Dt} - \nabla (\rho D_i \nabla Y_i) = w_i \qquad i \neq N \tag{7}$$

$$\rho \frac{Dh}{Dt} - \nabla \left\{ \lambda \nabla T + \sum_{i=1}^{N-1} \rho D_i (h_i - h_N) \nabla Y_i \right\} = -\rho \phi_r \tag{8}$$

The assumptions underlying Eqs. (7) and (8) are many, but they are usually necessary to make combustion problems tractable.[14] Possibly the most serious approximations in the present case are the use of Fick's law, Eqs. (6), in a multicomponent mixture and the neglect of thermal diffusion. As is discussed later, it may be possible to rework the problem with these restrictions removed. The form of Eq. (8) is unusual but it is the correct form, consistent with the Fick's law assumption for dilute species.

Element mass fractions Z_m for element m may be defined

$$Z_m \equiv \sum_{i=1}^{N} \mu_{m,i} Y_i \tag{9}$$

where $\mu_{m,i}$ is the mass fraction of element m in species i. Equation (7) may be weighted by $\mu_{m,i}$ and summed to yield

$$\rho \frac{DZ_m}{Dt} - \nabla \left\{ \rho \sum_{i=1}^{N-1} (\mu_{m,i} - \mu_{m,N}) D_i \nabla Y_i \right\} = 0 \tag{10}$$

since

$$\sum_{i=1}^{N} \mu_{m,i} w_i = 0$$

as elements are conserved under chemical reaction.

We consider a two-source (or stream) mixing problem in which the unmixed sources (or inlet streams) are denoted by the subscripts 1 and 2. We have then

$$Z_m(x,t) = Z_{m,2} + (\xi + z_m)(Z_{m,1} - Z_{m,2}) \tag{11}$$

$$h = h_2 + \xi(h_1 - h_2) + z_h Q \tag{12}$$

where $\xi(x,t)$ is a mixture fraction based on one of the elements (so that $z_m = 0$ for that element) and $z_m(x,t)$ and $z_h(x,t)$ are perturbations for element m and the enthalpy. In the absence of differential diffusion, z_m and z_h are zero and ξ is the universal mixture fraction. In some applications of interest, $h_1 \approx h_2$; thus $h_1 - h_2$ is not an appropriate scale for the enthalpy perturbation z_h. The scale Q may be arbitrarily chosen and is taken here as the heat of combustion per unit mass of stoichiometric combustion products.

The idea is to substitute Eqs. (11) and (12) into Eqs. (10) and (8), respectively, and derive equations for the perturbations z_m and z_h as well as the equation for ξ. This can be done for a system with any number of elements. Here we shall

confine ourselves to the hydrogen/oxygen/nitrogen system. We take hydrogen element as the basis for ξ and then only z_0 for oxygen need be determined since the mass fraction of nitrogen element is obtained by difference. The mixture is then described entirely by ξ and z_0, which determine its elemental composition, and by z_h, which, together with ξ, determines its enthalpy. If the chemical kinetic rates are very fast compared to the rate of turbulent mixing, then the molecular species and temperature will be everywhere the chemical equilibrium values for that elemental composition and enthalpy. This will be closely approximated for the hydrogen/oxygen/nitrogen system of interest here.[5,16] We have then that

$$Y_i = Y_i^0(\xi, z_0, z_h) \tag{13}$$

$$T = T^0(\xi, z_0, z_h) \tag{14}$$

where the superscript 0 denotes chemical equilibrium. Also

$$\nabla Y_i = \frac{\partial Y_i^0}{\partial \xi} \nabla \xi + \frac{\partial Y_i^0}{\partial_0} \nabla z_0 + \frac{\partial Y_i^0}{\partial z_h} \nabla z_h \tag{15}$$

$$\nabla T = \frac{\partial T^0}{\partial \xi} \nabla \xi + \frac{\partial T^0}{\partial z_0} \nabla z_0 + \frac{\partial T^0}{\partial z_h} \nabla z_h \tag{16}$$

These may be substituted into Eqs. (10) and (8) along with Eqs. (11) and (12) to yield after some manipulation

$$\rho \frac{D\xi}{Dt} - \nabla \cdot (\rho D_{\xi\xi} \nabla \xi) = \nabla \cdot (\rho D_{\xi 0} \nabla z_0) + \nabla \cdot (\rho D_{\xi h} \nabla z_h) \tag{17}$$

$$\rho \frac{Dz_0}{Dt} - \nabla \cdot (\rho D_{00} \nabla z_0) = \nabla \cdot (\rho D_{0\xi} \nabla \xi) + \nabla \cdot (\rho D_{0h} \nabla z_h) \tag{18}$$

$$\rho \frac{Dz_h}{Dt} - \nabla \cdot (\rho D_{hh} \nabla z_h) = \nabla \cdot (\rho D_{h\xi} \nabla \xi)$$

$$+ \nabla \cdot (\rho D_{h0} \nabla z_0) - \rho\phi \tag{19}$$

where

$$D_{\xi\xi} \equiv \sum_{i=1}^{N-1} \hat{\mu}_{H,i} D_i \frac{\partial Y_i^0}{\partial \xi}, \quad D_{\xi 0} \equiv \sum_{i=1}^{N-1} \hat{\mu}_{H,i} D_i \frac{\partial Y_i^0}{\partial z_0}$$

$$D_{\xi h} \equiv \sum_{i=1}^{N-1} \hat{\mu}_{H,i} D_i \frac{\partial Y_i^0}{\partial z_h}, \quad D_{00} \equiv \sum_{i=1}^{N-1} (\hat{\mu}_{0,i} - \hat{\mu}_{H,i}) D_i \frac{\partial Y_i^0}{\partial z_0}$$

$$D_{0\xi} \equiv \sum_{i=1}^{N-1} (\hat{\mu}_{0,i} - \hat{\mu}_{H,i}) D_i \frac{\partial Y_i^0}{\partial \xi}$$

$$D_{0h} \equiv \sum_{i=1}^{N-1} (\hat{\mu}_{0,i} - \hat{\mu}_{H,i}) D_i \frac{\partial Y_i^0}{\partial z_h}$$

$$\tag{20}$$

$$D_{hh} \equiv \sum_{i=1}^{N-1} \frac{D_i}{Q} [h_i - h_N - \hat{\mu}_{H,i}(h_1 - h_2)] \frac{\partial Y_i^0}{\partial z_h} + \frac{\lambda}{\rho Q} \frac{\partial T^0}{\partial z_h}$$

$$D_{h\xi} \equiv \sum_{i=1}^{N-1} \frac{D_i}{Q} [h_i - h_N - \hat{\mu}_{H,i}(h_1 - h_2)] \frac{\partial Y_i^0}{\partial \xi} + \frac{\lambda}{\rho Q} \frac{\partial T^0}{\partial \xi}$$

$$D_{h0} \equiv \sum_{i=1}^{N-1} \frac{D_i}{Q} [h_i - h_N - \hat{\mu}_{H,i}(h_1 - h_2)] \frac{\partial Y_i^0}{\partial z_0} + \frac{\lambda}{\rho Q} \frac{\partial T^0}{\partial z_0}$$

$$\phi \equiv \phi_r / Q$$

In the above

$$\hat{\mu}_{H,i} = \mu_{H,i}/(Z_{H,1} - Z_{H,2}), \quad \hat{\mu}_{0,i} = \mu_{0,i}/(Z_{0,1} - Z_{0,2})$$

and the partial derivatives are evaluated at the local values of ξ, z_0, and z_h.

To reduce the size of the computational task we here introduce some linearizations. We assume that z_0 and z_h are small so that extraneous terms in Eqs. (17-19) may be dropped, yielding

$$\rho \frac{D\xi}{Dt} - \nabla \cdot (\rho D_{\xi\xi} \nabla \xi) = 0 \tag{21}$$

$$\rho \frac{Dz_0}{Dt} - \nabla \cdot (\rho D_{00} \nabla z_0) = \nabla \cdot (\rho D_{0\xi} \nabla \xi) \tag{22}$$

$$\rho \frac{Dz_h}{Dt} - \nabla \cdot (\rho D_{hh} \nabla z_h) = \nabla \cdot (\rho D_{h\xi} \nabla \xi) - \rho\phi \tag{23}$$

and the partial derivatives appearing in Eqs. (20) are then evaluated at $\xi = \xi$, $z_0 = 0$, $z_h = 0$. Furthermore, Eqs. (13) and (14) can be linearized

$$Y_i = Y_i^0(\xi, 0, 0) + \frac{\partial Y_i^0}{\partial z_0} z_0 + \frac{\partial Y_i^0}{\partial z_h} z_h \tag{24}$$

$$T = T^0(\xi, 0, 0) + \frac{\partial T^0}{\partial z_0} z_0 + \frac{\partial T^0}{\partial z_h} z_h \tag{25}$$

with derivatives here also evaluated at $\xi = \xi$, $z_0 = 0$, $z_h = 0$.

Equations (21-23) are of the same form as Eqs. (6) and (7) of the earlier paper[13] and may be averaged and modeled in a similar way to that paper. We use density-weighted, or Favre, averaging; the axisymmetric boundary layer form of the equations; and the $k - \epsilon$ (Ref. 17) model for the turbulence. Equations for $\tilde{\xi}$, $\widetilde{\xi''^2}$, $\tilde{z}_0$, $\widetilde{z_0''^2}$, $\tilde{z}_h$, $\widetilde{z_h''^2}$, $\widetilde{\xi''z_0''}$, $\widetilde{\xi''z_h''}$, $\widetilde{z_0''z_h''}$ result:

$$\bar{\rho}\tilde{u}\frac{\partial\tilde{\xi}}{\partial x} + \bar{\rho}\tilde{v}\frac{\partial\tilde{\xi}}{\partial r} - \frac{1}{r}\frac{\partial}{\partial r}\left\{\bar{\rho}r\left(\frac{\nu_T}{\sigma_\xi} + \tilde{D}_{\xi\xi}\right)\frac{\partial\tilde{\xi}}{\partial r}\right\} = 0 \tag{26}$$

$$\bar{\rho}\tilde{u}\frac{\partial\widetilde{\xi''^2}}{\partial x} + \bar{\rho}\tilde{v}\frac{\partial\widetilde{\xi''^2}}{\partial r} - \frac{1}{r}\frac{\partial}{\partial r}\left\{\bar{\rho}r\left(\frac{\nu_T}{\sigma_g} + \tilde{D}_{\xi\xi}\right)\frac{\partial\widetilde{\xi''^2}}{\partial r}\right\}$$

$$= \bar{\rho}C_{g_1}\nu_T\left(\frac{\partial\tilde{\xi}}{\partial r}\right)^2 - C_{g_2}\bar{\rho}\frac{\epsilon}{k}\widetilde{\xi''^2} \tag{27}$$

$$\bar{\rho}\tilde{u}\frac{\partial\tilde{z}_k}{\partial x} + \bar{\rho}\tilde{v}\frac{\partial\tilde{z}_k}{\partial r} - \frac{1}{r}\frac{\partial}{\partial r}\left\{\bar{\rho}r\left(\frac{\nu_T}{\sigma_z} + \tilde{D}_{kk}\right)\frac{\partial\tilde{z}_k}{\partial r}\right\}$$

$$= \frac{1}{r}\frac{\partial}{\partial r}\left\{\bar{\rho}rD_{k\xi}\frac{\partial\tilde{\xi}}{\partial r}\right\} - \delta_{hk}\bar{\rho}\tilde{\phi} \tag{28}$$

$$\bar{\rho}\tilde{u}\frac{\partial\widetilde{z_k''^2}}{\partial x} + \bar{\rho}\tilde{v}\frac{\partial\widetilde{z_k''^2}}{\partial r} - \frac{1}{r}\frac{\partial}{\partial r}\left\{\bar{\rho}r\left(\frac{\nu_T}{\sigma_{zz}} + \tilde{D}_{kk}\right)\frac{\partial\widetilde{z_k''^2}}{\partial r}\right\}$$

$$= \bar{\rho}C_{g_1}\nu_T\left(\frac{\partial\tilde{z}_k}{\partial r}\right)^2 - \bar{\rho}C_{g_2}\frac{\epsilon}{k}\widetilde{z_k''^2} - \delta_{hk}\overline{\rho z_k''\phi''} \tag{29}$$

$$\bar{\rho}\tilde{u}\frac{\partial\widetilde{\xi''z_k''}}{\partial x} + \bar{\rho}\tilde{v}\frac{\partial\widetilde{\xi''z_k''}}{\partial r} - \frac{1}{r}\frac{\partial}{\partial r}\left\{\bar{\rho}r\left(\frac{\nu_T}{\sigma_{\xi z}} + \frac{\tilde{D}_{\xi\xi} + \tilde{D}_{kk}}{2}\right)\frac{\partial\widetilde{\xi''z_k''}}{\partial r}\right\}$$

$$= \bar{\rho}C_{g_1}\nu_T\frac{\partial\tilde{\xi}}{\partial r}\frac{\partial\tilde{z}_k}{\partial r} - \bar{\rho}C_{g_2}\frac{\epsilon}{k}\widetilde{\xi''z_k''} - \delta_{hk}\bar{\rho}\widetilde{\xi''\phi''} \tag{30}$$

$$\bar{\rho}\tilde{u}\frac{\partial\widetilde{z_0''z_h''}}{\partial x} + \bar{\rho}\tilde{v}\frac{\partial\widetilde{z_0''z_h''}}{\partial r} - \frac{1}{r}\frac{\partial}{\partial r}\left\{\bar{\rho}r\left(\frac{\nu_T}{\sigma_{\xi z}} + \frac{\tilde{D}_{00} + \tilde{D}_{hh}}{2}\right)\frac{\partial\widetilde{z_0''z_h''}}{\partial r}\right\}$$

$$= \bar{\rho}C_{g_1}\nu_T\frac{\partial\tilde{z}_0}{\partial r}\frac{\partial\tilde{z}_h}{\partial r} - \bar{\rho}C_{g_2}\frac{\epsilon}{k}\widetilde{z_0''z_h''} - \bar{\rho}\widetilde{z_0''\phi''} \tag{31}$$

where the subscript k denotes either of the subscripts 0 or h in Eqs. (28-30). The parameters σ_z, $\sigma_{\xi z}$, σ_{zz} are turbulent Schmidt numbers and the model constants C_{g_1} and C_{g_2} are taken as the same in each equation. There are certain problems associated with the modeling of the dissipation terms in Eqs. (29-31). These are discussed in the earlier paper.[13] They require resolution by reference to experiment. The correlations with the radiant loss rate have not been modeled as yet.

Equations (26 – 31) may be solved in parallel with equations for the mean velocity $\bar{u}$, turbulence kinetic energy k, and turbulence dissipation ϵ in the normal manner. Closure of the equations requires specification of the mean density in terms of ξ, z_0, z_h. In the present case this was done by the following linearizations

$$1/\rho = v_s(\xi) + a_v(\xi)z_0 + b_v z_h \qquad (32)$$

$$1/\bar{\rho} = \bar{v}_s + \tilde{a}_v \tilde{z}_0 + b_v \tilde{z}_h \qquad (33)$$

where $v_s(\xi)$ is the specific volume in the absence of differential diffusion and

$$a_v(\xi) \equiv \frac{\partial(1/\rho)}{\partial z_0} \qquad (34)$$

$$b_v \equiv \frac{\partial(1/\rho)}{\partial z_h} = \frac{\gamma-1}{\gamma} \frac{Q}{P} \qquad (35)$$

with γ being the ratio of the equilibrium specific heats. It is found that b_v is largely independent of ξ. The Favre averaging of v_s and a_v is done in the normal manner using the Favre probability density function for ξ.

Boundary conditions for $\tilde{z}_k$, $\widetilde{z_k''^2}$, $\widetilde{\xi''z_k''}$, and $\widetilde{z_0''z_h''}$ are that they have zero value in the two inlet streams and a zero normal derivative at the axis of symmetry. Nonzero values for $\tilde{z}_k$ arise from the source term on the right-hand side of Eq. (27) and gradients in $\tilde{z}_k$ give rise to the variances and covariances.

Property Data for the Hydrogen/Air System

The diffusion coefficients appearing in Eqs. (21-23) and defined in Eqs. (20) were determined in the following manner. The species diffusivities were assumed to be those into nitrogen and these were obtained from power law fits to the Chapman-Enskog theory derived by Mitchell[19]:

$$D_i = D_{i,N_2} = fT^{1.67}/P \, \mathrm{cm}^2/\mathrm{s}$$

Similar fits to the thermal conductivity of component gases as derived by Mitchell[19] were also used:

$$\lambda_i = cT^\alpha \, \mathrm{cal/cm\text{-}s\text{-}K}$$

These were mole fraction weighted to obtain the overall thermal conductivity. Molecular viscosities were also determined for each species from Mitchell's fits:

$$\mu_i = eT^{0.6756} \, \mathrm{g/cm\text{-}s}$$

and the overall viscosity (used in the momentum equation model) determined by mole fraction weighting. In all cases T is in Kelvin and the pressure P is in atmospheres. The constants for the fits are given in Table 1. The mole weighting of viscosity and thermal conductivity are gross approximations but are consistent with the treatment of the mass diffusivities.

The density, temperature, and composition were obtained as a function of the mixture fraction (mass fraction of hydrogen fuel, z_0 and z_h zero) by calculation for adiabatic,

Table 1   Constants used in fits for diffusivity, thermal conductivity, and viscosity.[19] $D_i = fT^{1.67}/P$ cm^2/s; $\lambda_i = cT^\alpha$ cal/cm-s-K; $\mu_i = eT^{0.6756}$ g/cm-s

Species i	$f \times 10^5$	$c \times 10^7$	d	$e \times 10^6$
H	8.171	137.2	0.6484	1.5426
H$_2$	5.525	51.84	0.7681	1.8405
OH	2.030	14.804	0.7601	4.115
H$_2$O	1.905	0.8304	1.1748	0.5083
N$_2$	1.488	7.6893	0.7722	3.6974
O	2.076	22.219	0.6547	4.0387
O$_2$	1.523	7.1352	0.7968	4.4203
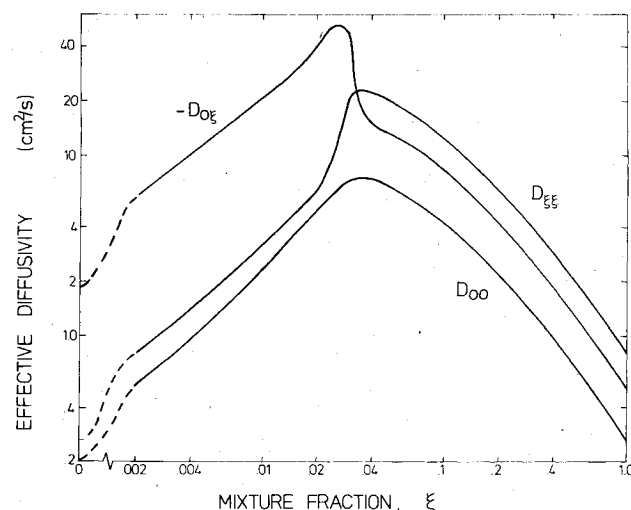
Fig. 1   Effective diffusivities for hydrogen and oxygen elements.

equilibrium reaction with dry air using the program of Gordon and McBride[20] and the derivatives with respect to ξ being determined by finite-difference techniques. Enthalpies of individual species were obtained from the JANAF tables.[21] Partial derivatives with respect to z_0 and z_h required for the derivatives in Eqs. (20), (24), (25), (34), and (35) were obtained by finite-difference techniques after running the Gordon and McBride[20] adiabatic equilibrium calculation for several values of the oxygen content and the temperature of the air. In one case this was not necessary, as

$$\frac{\partial T}{\partial z_h} \equiv \frac{Q}{c_p^e}$$

where c_p^e is the equilibrium specific heat of the mixture. The enthalpy scale factor Q is arbitrarily chosen as the heat of reaction per unit mass of stoichiometric mixture and is equal to 811.4 cal/g.

The diffusivities $D_{\xi\xi}$, $D_{0\xi}$, and D_{00} are shown in Fig. 1. Algebraic fits to these as used in the numerical integration are shown in Table 2. It can be seen that $D_{\xi\xi}$, which can be interpreted as the effective diffusivity for hydrogen element, reaches quite high values just on the rich side of stoichiometric, which occurs at $\xi = \xi_s = 0.0283$. It is seen that on the lean side of stoichiometric this diffusivity is 2-5 times the kinematic viscosity (shown in Fig. 3 and Table 2). This low effective molecular Schmidt number may have implications for the turbulence structure in the outer part of the flame at low Reynolds number. The differential diffusivity $D_{0\xi}$ can be interpreted as the difference between the diffusivity of oxygen and hydrogen element. It is negative over the whole range, indicating that the diffusivity of oxygen element is lower than that for hydrogen element. More than that, it can be seen that on the lean side of stoichiometric ($\xi < 0.033$, in fact) the effective diffusivity for oxygen element ($D_{0\xi} + D_{\xi\xi}$) is negative,

Table 2 Algebraic fits to property data

Property	Units	Range of ξ	Formula
$D_{\xi\xi}$	cm^2/s	$0 \le \xi \le 0.0325$	$D_{\xi\xi} = 0.26 + 257\xi + 3.5 \times 10^8 \xi^5$
		$0.0325 < \xi \le 1$	$D_{\xi\xi} = 3.8 - 3.03\xi + 27.5(1.0001 - \xi)^{10}$
$D_{0\xi}$	cm^2/s	$0 \le \xi \le 0.025$	$D_{0\xi} = -1.83 - 2000\xi$
		$0.025 < \xi \le 1$	$D_{0\xi} = -0.51 - 0.385(\xi^{-1.3} - 1)$
D_{00}	cm^2/s	$0 \le \xi \le 0.03$	$D_{00} = 0.21 + 206.7\xi + 1778\xi^2$
		$0.03 < \xi \le 1$	$D_{00} = 1.261 - \xi + 9.215(1.0001 - \xi)^{9.5}$
$D_{h\xi}$	cm^2/s	$0 \le \xi \le 0.020$	$D_{h\xi} = -2.5 - 575\xi - 52,800\xi^2 + 1.049 \times 10^{10} \xi^5$
		$0.02 < \xi \le 0.035$	$D_{h\xi} = -13 + 145 \exp\{ -14860(\xi - 0.033)^2 \}$
		$0.035 < \xi \le 1$	$D_{h\xi} = -3.93 - 58(1.0001 - \xi)^3 + 1.25\xi^{-1.475}$
D_{hh}	cm^2/s	$0 \le \xi \le 0.048$	$D_{hh} = 0.214 + 150\xi + 8182\xi^2 - 5.096 \times 10^7 \xi^5$
		$0.048 < \xi \le 1$	$D_{hh} = 7.39 - 6\xi + 9.88(1.0001 - \xi)^{5.34}$
ν	cm^2/s	$0 \le \xi \le 0.0265$	$\nu = 0.154 + 150.9\xi$
		$0.0265 < \xi \le 1$	$\nu = 1.96 - 0.9\xi + 2.68(1.0001 - \xi)^{6.8}$
v_s	m^3/kg	$0 \le \xi \le 0.0275$	$v_s = 0.845 + 335.3\xi - 2830\xi^2$
		$0.0275 < \xi \le 0.4$	$v_s = 6 + 6.36(\xi - 0.0245)^{0.208}$
		$0.4 < \xi \le 1$	$v_s = 10.4 + 1.76\xi$
a_v	m^3/kg	$0 \le \xi \le 0.03$	$a_v = 0.0254 + 4\xi + 1.925 \times 10^7 \xi^5 - 6.173 \times 10^{21} \xi^{14}$
		$0.03 < \xi \le 1$	$a_v = -9.8 + 0.1314(\xi + 0.025)^{-1.39}$
ϕ	s^{-1}	$0 \le \xi \le 0.033$	$\phi = 2.97 \exp\{ -6172.8(0.031 - \xi)^2 \}$
		$0.033 < \xi \le 1$	$\phi = 12.3(1 - \xi^2)^{6.7}$
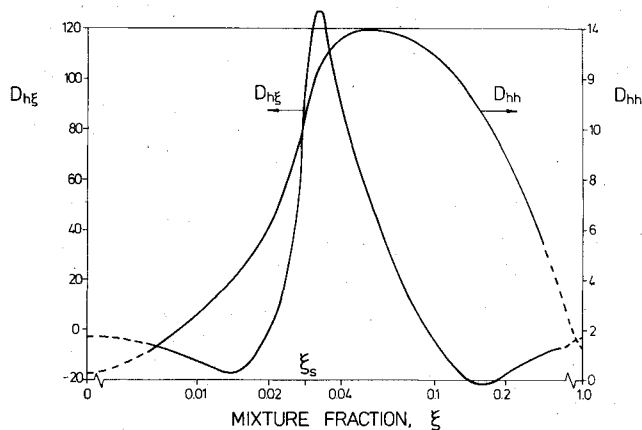
Fig. 2 Effective diffusivities for enthalpy.
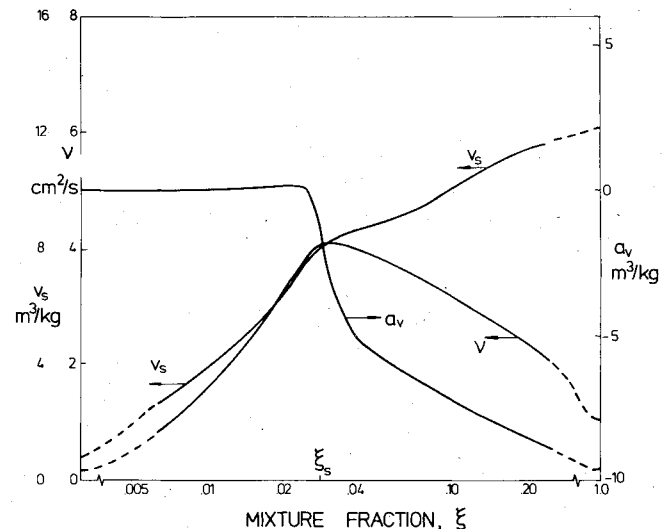
Fig. 3 Kinematic viscosity, specific volume, and influence coefficient of oxygen differential diffusion on specific volume.

indicating that oxygen element diffusion is counter to the gradient. This arises from the fact that the diffusivity of H_2O is greater than that for O_2. The radicals H and OH make very significant but not dominant contributions near stoichiometric. The neglect of superequilibrium radical concentrations (due to finite rate kinetics[16]) may be a significant overall contribution at moderate to low Damkohler number.

The diffusivities $D_{h\xi}$ and D_{hh} are shown in Fig. 2, and algebraic fits to them are given in Table 2. It is seen that $D_{h\xi}$ is positive near stoichiometric but is negative outside this range. This complex behavior should give rise to some interesting effects on the flame temperature. The values of the diffusivities shown are very large compared with the kinematic viscosity. It should be remembered that the scaling for $D_{h\xi}$ and D_{hh} is arbitrary since it depends on the value of Q. However, the choice of Q as the heat release per unit mass of combustion products should mean that these diffusivities are the effective thermal diffusivity operating on the flame to air temperature difference.

Figure 3 shows the kinematic viscosity ν and the specific volume functions v_s and a_v defined in Eqs. (32) and (34). Algebraic fits are once again shown in Table 2. It is seen that a_v undergoes a very strong variation, its large negative value on the rich side of stoichiometric being due to the very strong effect of a decrease of elemental oxygen on the flame temperature. On the other hand, b_v was found to vary from 9.57 m^3/kg at $\xi = 0$ and 1, dipping to a minimum of 5.1 m^3/kg at

$\xi = 0.03$. Such variation is of second order and an average value of $b_v = 7.3$ m^3/kg has been used in the calculation.

The radiative loss rate term ϕ was calculated from the absorptivity of water vapor[22] using $X^0_{H_2O}$ and T^0, assuming the flame to be optically thin. A functional fit with ξ has been determined as shown in Table 2.

In converting the computational results in terms of z_0 and z_h to the effects on species concentration and temperature, it is necessary to use the functions and derivatives that appear in Eqs. (24) and (25). Figure 4 gives these for temperature and Figs. 5 and 6 for nitrogen and hydrogen, respectively. Results for other species can also be obtained as well as for combined variables such as nitric oxide formation rate.

Results

Numerical solutions of Eqs. (26-28) have been carried out using the finite-difference computer program and methodology reported earlier.[18] Turbulence model constants have been kept the same, and the turbulent Schmidt number σ_z is taken as 0.7. The special model for low Reynolds number turbulence of Jones and Launder[17] has been included in the modeled equations for velocity, turbulence kinetic energy, and dissipation, which are solved simultaneously. The
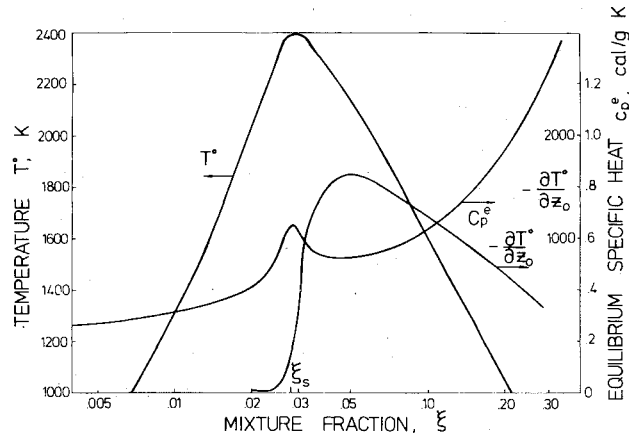
Fig. 4 Temperature, equilibrium specific heat, and influence coefficient of oxygen differential diffusion on temperature.
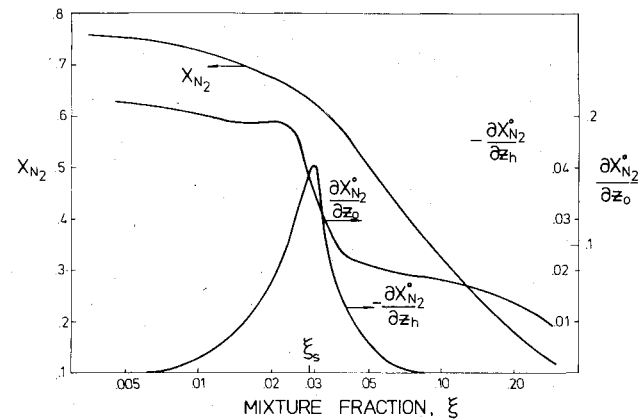

Fig. 5 Nitrogen mole fraction and influence coefficients for differential diffusion of oxygen and enthalpy.
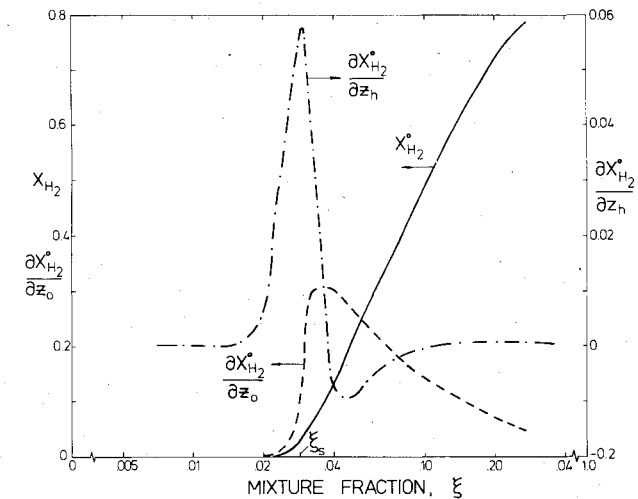

Fig. 6 Hydrogen mole fraction and influence coefficients for differential diffusion of oxygen and enthalpy.

solution procedure uses a simple model[18] for the probability density function of ξ involving a clipped Gaussian distribution plus an intermittent spike. The intermittency is found from an empirical correlation dependent on the mean and variance of ξ. This pdf is used to weight the property data shown in Table 2 to obtain the necessary averages $\bar{D}_{\xi\xi}$, $\bar{D}_{0\xi}$, $\bar{\nu}$, $\bar{\rho}$, etc.

Calculations have been made for the flame of Drake et al.[6] in which a jet of hydrogen 3.2-mm in diameter exists with a
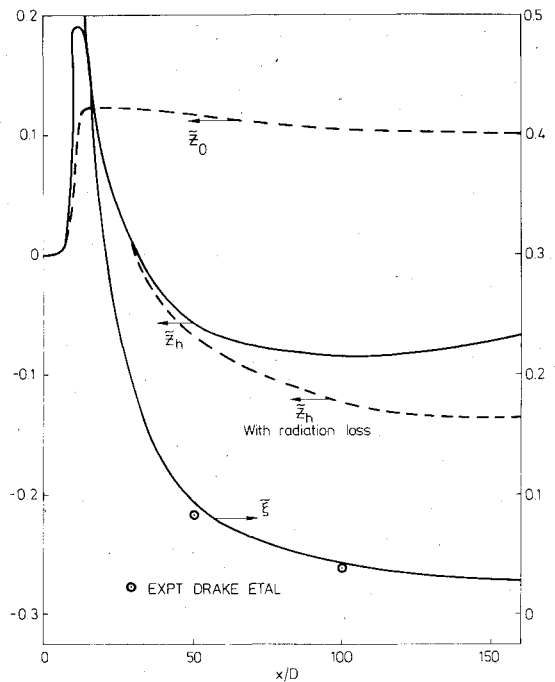
Fig. 7 Results for mixture fraction and its perturbations on centerline of hydrogen/air diffusion flame of Drake et al.[6]

mean velocity of 50 m/s into a coflowing stream of air with a velocity of 10 m/s. Information is available on the initial velocity and turbulence profiles, and on the axial pressure gradient in the tunnel.[23] The dissipation length scale $L_\epsilon \equiv k^{3/2}/\epsilon$ is arbitrarily chosen at 0.2 times the jet diameter. Computations have been made with and without radiative loss.

Figure 7 shows results for $\bar{\xi}$, $\bar{z}_h$, and $\bar{z}_0$ along the centerline of this flame. It is seen that $\bar{z}_0$ and $\bar{z}_h$ are quite large and that linearizations of Eqs. (21-26) and (33) are not justified in this flame. (Such linearizations will of course be justified in flames of higher Reynolds number, where $\bar{z}_0$ and $\bar{z}_h$ will be much smaller.) It is seen that $\bar{z}_h$ is positive near the jet exit and is negative further downstream. This can be ascribed to the fact that $\bar{D}_{h\xi}$ near the centerline is negative near the jet and positive downstream. Figure 8 shows the radial variation at x/D of 55. (D is here the jet diameter and $a = D/2$.) Table 3 lists the various diffusivities across the flow at $x/D = 55$.

The change of sign of $\bar{z}_0$ in the outer part of the profile is related to the change in sign of $\partial^2\bar{\xi}/\partial r^2$ and is necessary to conserve a zero total flux of $\bar{z}_0$ when integrated across the flow. This necessary condition forms a good check on the numerical accuracy of the computation, and in our case the flux of z_0 was less than 10^{-3} of the flux of ξ up to x/D of 100. A similar result for this check is obtained for $\bar{z}_h$ in the no radiation case. The estimation formula, Eq. (1), with d here as $\bar{D}_{k\xi}$, $D = \bar{D}_{kk}$, and $D_T = \nu_T/0.7$ gives order of magnitude estimates for $\bar{z}_0$ and $\bar{z}_h$ on the centerline, with a constant of proportionality of 0.5 and 0.2 when the diffusivities are calculated in the middle of the shear layer ($\xi/\xi_0 = 0.5$) and ξ_0 is the value of ξ at the centerline. These can be compared with the value of 0.5 found in the much simpler nonreacting flow case.[13]

Comparison of the computed flame field with the measurements of Drake et al.[6] indicates that the computed flame is about 10% longer than the actual flame. The agreement obtained is really quite good considering the reservations one must have about the use of the $k-\epsilon$ model in such a variable density flow and that the low Reynolds number effects on the turbulence are quite large. Table 3 shows that in the middle of the shear layer the turbulence Reynolds number ($Re_t \equiv k^2/\nu\epsilon$) is about 40. This reduces C_μ,

Table 3 Mean diffusivities and other variables across the flame shear layer at $x/D = 55$

r/a	0	2.95	4.44	6.27	8.13
$\bar{\xi}/\xi_0$	1.0	0.788	0.581	0.279	0.028
$(\bar{u}-u_e)/(u_c-u_e)$	1.0	0.584	0.118	−0.052	−0.044
$\bar{D}_{\xi\xi}$ cm^2/s	15.4	17.8	20.2	9.3	0.86
$\bar{D}_{0\xi}$ cm^2/s	−10.5	−14.5	−21.5	−41.8	−6.5
$\bar{D}_{00}$ cm^2/s	5.3	6.1	7.0	5.9	0.71
$\bar{D}_{h\xi}$ cm^2/s	4.1	24.8	63.5	32.5	−4.2
$\bar{D}_{hh}$ cm^2/s	13.2	13.9	14.0	7.6	0.63
$\bar{\nu}$ cm^2/s	3.4	3.6	3.9	3.5	0.51
ν_T cm^2/s	8.4	3.9	0.18	0.02	0.03
Re_t	67.8	49.7	14.3	1.89	7.1
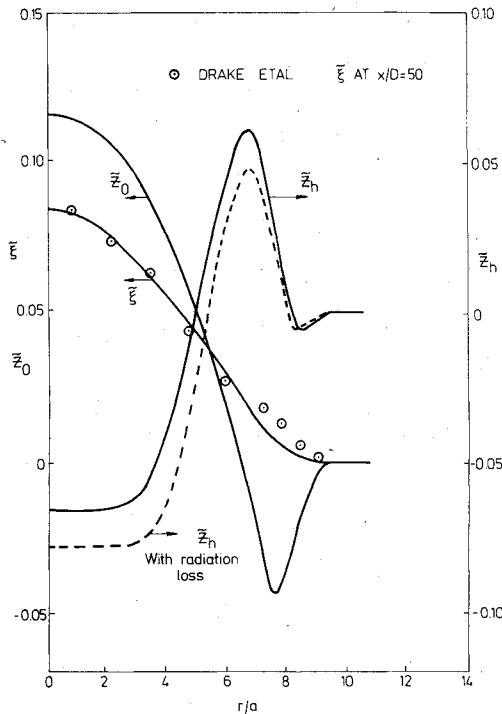
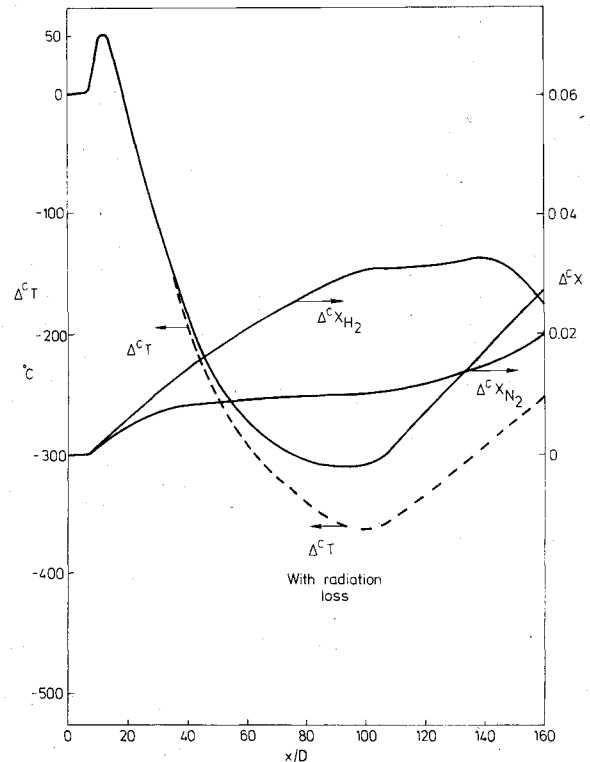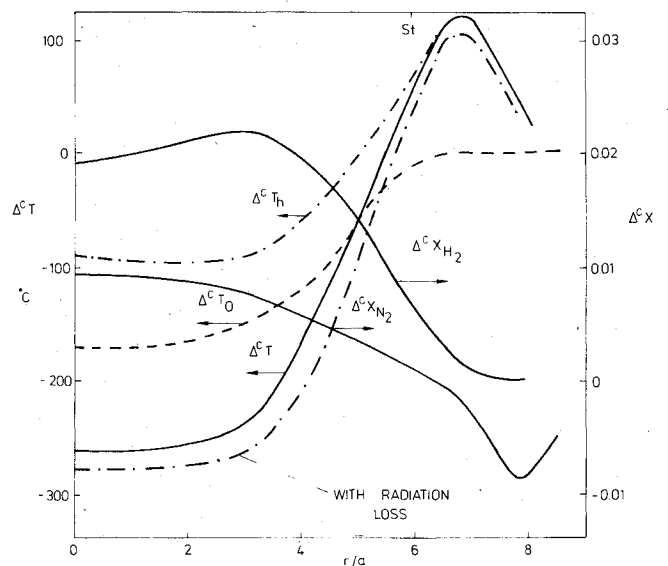Fig. 8 Radial variation of mixture fraction and its perturbations at x/D of 55.

Fig. 9 Characteristic departures of temperature and molecular nitrogen and hydrogen mole fraction due to differential diffusion on flame centerline.

Fig. 10 Characteristic departures of temperature and mole fraction across the flame at $x/D = 55$.
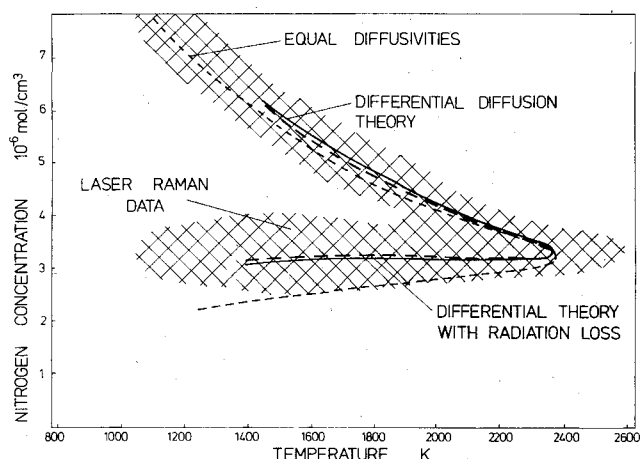
the coefficient in the turbulent viscosity model, by a factor of about 3 with consequent reduction of turbulence levels and the rate of flame spread.

The effects of differential diffusion on the molecular species concentrations and temperature could be obtained by weighting the linearized Eqs. (23) and (24) by the joint pdf for ξ, z_0, and z_h. This would give average temperatures and concentrations and average departures from the equal diffusivity relations represented by the lead terms in those equations. The computations carried out to date do not give us enough information to compute this joint pdf. For our present purposes it will be sufficient to calculate characteristic temperature and mole fraction departures defined by

$$\Delta^c T \equiv \left(\frac{\partial T^0}{\partial z_0}\right)_\xi \bar{z}_0 + \left(\frac{\partial T^0}{\partial z_h}\right)_\xi \bar{z}_h \qquad (37)$$

$$\Delta^c X_i \equiv \left(\frac{\partial X_i^0}{\partial z_0}\right)_\xi \bar{z}_0 + \left(\frac{\partial X_i^0}{\partial z_h}\right)_\xi \bar{z}_h \qquad (38)$$

the influence coefficients $\partial T^0/\partial z_k$ and $\partial X_i^0/\partial z_k$ being computed at $\bar{\xi}$. Figures 9 and 10 show these characteristic temperature and mole fraction departures on the centerline and across the flame at $x/D = 40$. It is seen that the tem-

Fig. 11 Predicted effect of differential diffusion on correlation of temperature and hydrogen concentration; experimental data of Drake et al.[6]
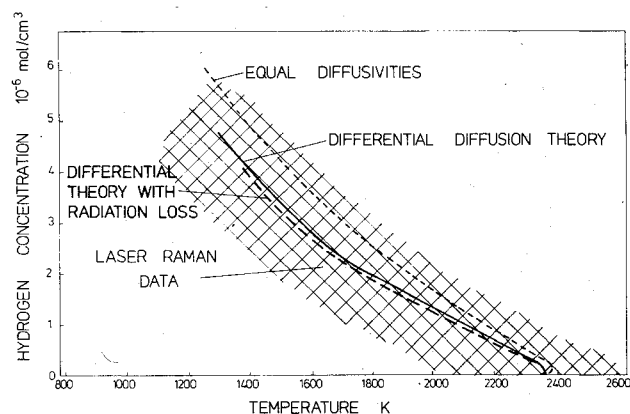

Fig. 12 Predicted effect of differential diffusion on correlation of temperature and hydrogen concentration; experimental data of Drake et al.[6]

perature departures are very large indeed. They are an order of magnitude larger than the average temperature departures found for chemical nonequilibrium.[16] It is apparent that the departures will still be substantial in the flame that we have been studying at Sydney University.[9,11,24] There could be significant effects on nitric oxide formation. Figure 10 shows the breakdown of the temperature departure into its components arising from the differential diffusion of oxygen element $\Delta^c T_0$, the first term in Eq. (37), and that due to enthalpy $\Delta^c T_h$, the second term in Eq. (37). It is seen that oxygen element diffusion is the dominant feature on the rich side of the flame. For the species mole fractions the effect is almost all due to the oxygen element differential diffusion.

Figures 11 and 12 show these results plotted as correlation diagrams between temperature and concentration. The differential diffusion theory curves shown are for temperature computed as

$$T(\tilde{\xi}) \equiv T^0(\tilde{\xi}) + \Delta^c T(\tilde{\xi}) \tag{39}$$

cross-plotted vs concentration computed as

$$C_i(\tilde{\xi}) \equiv \frac{P}{\hat{R}} \frac{X_i^0(\tilde{\xi}) + \Delta^c X_i(\tilde{\xi})}{T^0(\tilde{\xi}) + \Delta^c T(\tilde{\xi})} \tag{40}$$

where P is the pressure and $\hat{R}$ the universal gas constant. The equal diffusivity theory curves are then simply Eqs. (39) and (40) cross-plotted with $\Delta^c T$ and $\Delta^c X_i$ set equal to zero. The

cross-plotting is done from the data obtained across the flame at $x/D = 55$. This is shown compared with the data of Drake et al.[6] at $x/D = 50$, which is the comparable station since the computations give a longer flame. The cross-plot correlation is not very sensitive to x/D in this part of the flame. It can be seen that the agreement is, in general, very good, the differential diffusion theory lying much closer to the middle of the measured data than for the equal diffusivity theory. The wide scatter of the data is due partly to the Poisson statistics of the measurement method but is also due to turbulence. In the absence of differential diffusion and measurement errors, all points should lie on the equal diffusivity curve. With differential diffusion, such perfect correlation would only occur if the fluctuations in z_0 and z_h are perfectly correlated with ξ. It is proposed to calculate these correlations and compare them with the more recent measurements of Drake et al.[7]

Although the agreement between theory and experiment is most encouraging, this should be viewed against improvements needed in the theory to obtain really satisfactory predictions in this case. The linearizations involved in Eqs. (21-23) could easily be eliminated, but those involved in Eqs. (24) and (25) and the effective diffusivities are not so easily handled. The Fick's law assumption could be eliminated by solving the Stefan-Maxwell equations by using Eqs. (15), (16) and (14) and (13) so that new expressions for the effective diffusivities, Eqs. (20), are arrived at.

Conclusions

A theory for differential molecular transport in turbulent diffusion flames has been developed from fundamental principles. Effective differential diffusivities for elemental species and enthalpies have been derived and values computed for the hydrogen/air system. These values are found to be much larger than the kinematic viscosity, which is already large in such flames. Solutions of the turbulent form of the equations for the perturbations in element and enthalpy mixture fractions yield results which are in good agreement with laser Raman measurements in a low Reynolds number flame. The theory could be improved by eliminating some of the linearizations and avoiding the Fick's law assumption.

Acknowledgments

References

[1] Spalding, D. B., "Mathematische Modelle Turbulenter Flammen," *VDI Berichte,* Vol. 146, 1970, pp. 25-30.

[2] Bilger, R. W., "Turbulent Jet Diffusion Flames," *Progress in Energy and Combustion Science,* Vol. 1, 1976, pp. 87-109.

[3] Libby, P. A. and Williams, F. A., "Some Implications of Recent Theoretical Studies in Turbulent Combustion," *AIAA Journal,* Vol. 19, March 1981, pp. 261-274.

[4] Bilger, R. W., "The Structure of Diffusion Flames," *Combustion Science and Technology,* Vol. 13, 1976, pp. 155-170.

[5] Bilger, R. W., "Turbulent Flow with Nonpremixed Reactants," *Turbulent Reacting Flow,* edited by Libby, P. A. and Williams, F. A., *Topics in Applied Physics,* Vol. 44, Springer-Verlag, Heidelberg, 1980, pp. 65-113.

[6] Drake, M. C., Lapp, M., Penney, C. M., Warshaw, S., and Gerhold, B. W., "Measurements of Temperature and Concentration

Fluctuations in Turbulent Diffusion Flames Using Pulsed Raman Spectroscopy,'' Eighteenth Symposium (International) on Combustion, The Combustion Institute, Pittsburgh, Pa., 1981, pp. 1521-1531.

[7]Drake, M. C., Lapp, M., Penney, C. M., Warshaw, S., and Gerhold, B. W., "Probability Density Functions and Correlations of Temperature and Molecular Concentrations in Turbulent Diffusion Flames,'' AIAA Paper 81-0103, Jan. 1980.

[8]Miller, J. A. and Kee, R. J., "Chemical Nonequilibrium Effects in Hydrogen-Air Laminar Jet Diffusion Flames,'' *Journal of Physical Chemistry*, Vol. 81, 1977, pp. 2534-2542.

[9]Bilger, R. W. and Beck, R. E., "Further Experiments on Turbulent Jet Diffusion Flames,'' Fifteenth Symposium (International) on Combustion, The Combustion Institute, Pittsburgh, Pa., 1975, pp. 541-552.

[10]Becker, H. A., "Mixing, Concentration Fluctuations, and Marker Nephelometry,'' *Studies in Convection,* Vol. 2, edited by Launder, B. E., Academic Press, New York, 1977, pp. 45-139.

[11]Kennedy, I. M. and Kent, J. H., "Measurements of a Conserved Scalar in Turbulent Jet Diffusion Flames,'' Seventeenth Symposium (International) on Combustion, The Combustion Institute, Pittsburgh, Pa., 1979, pp. 279-287.

[12]Bilger, R. W., "On Diffusion and Reaction in Turbulent Shear Flows,'' Western States Section, The Combustion Institute, Pittsburgh, Pa., Paper WSS 80-1, April 1980.

[13]Bilger, R. W. and Dibble, R. W., "Differential Molecular Diffusion Effects in Turbulent Mixing and Combustion: I—Nonreacting Flow,'' Sandia National Laboratories, Livermore, Calif., Rept. SAND80-8809, Aug. 1981.

[14]Williams, F. A., *Combustion Theory,* Addison Wesley, Reading, Mass., 1965.

[15]Bird, R. B., Stewart, W. E., and Lightfoot, E. N., *Transport Phenomena,* John Wiley and Sons, New York, 1960.

[16]Bilger, R. W., "Perturbation Analysis of Turbulent Nonpremixed Combustion,'' *Combustion Science Technology,* Vol. 22, 1980, pp. 251-261.

[17]Jones, W. P. and Launder, B. E., "The Prediction of Laminarization with a Two-Equation Model of Turbulence,'' *International Journal of Heat and Mass Transfer,* Vol. 15, 1972, pp. 301-314.

[18]Kent, J. H. and Bilger, R. W., "The Prediction of Turbulent Diffusion Flame Fields and Nitric Oxide Formation,'' Seventeenth Symposium (International) on Combustion, The Combustion Institute, Pittsburgh, Pa., 1977, pp. 1643-1656.

[19]Mitchell, R. E., "A Theoretical Model of Chemically Reacting Recirculating Flows,'' Sandia National Laboratories, Livermore, Calif., Rept. SAND79-8236, April 1980.

[20]Gordon, A. S. and McBride, B., "Computer Program for Calculation of Complex Chemical Equilibrium Compositions, Rocket Performance, Incident and Reflected Shocks and Chapman-Jouget Detonations,'' NASA SP-273, 1971.

[21]Stull, D. R., et al., "JANAF Thermochemical Tables,'' Dow Chemical Co., Michigan, 1973.

[22]Hottel, H. C. and Sarofim, A. F., *Radiative Transfer,* McGraw-Hill, New York, 1967.

[23]Drake, M., personal communication, 1981.

[24]Kent, J. H. and Bilger, R. W., "Turbulent Diffusion Flames,'' Fourteenth Symposium (International) on Combustion, The Combustion Institute, Pittsburgh, Pa., 1973, pp. 615-625.